Catalysis Science & Technology

New Possibility of Hydroxyapatites as Noble-Metal-Free Catalyst towards Total Decomposition of Volatile Organic Compounds

Journal:	*Catalysis Science & Technology*
Manuscript ID	CY-ART-04-2020-000787.R1
Article Type:	Paper
Date Submitted by the Author:	18-May-2020
Complete List of Authors:	Xin, Yunzi; Nagoya Institute of Technology, Ando, Yuri; Nagoya Institute of Technology Nakagawa, Sohei; Nagoya Institute of Technology Nishikawa, Harumitsu; Nagoya Kogyo Daigaku, Shirai, Takashi; Nagoya Institute of Technology,

ARTICLE

New Possibility of Hydroxyapatites as Noble-Metal-Free Catalyst towards Total Decomposition of Volatile Organic Compounds

Received 00th January 20xx,
Accepted 00th January 20xx

DOI: 10.1039/x0xx00000x

Yunzi Xin,[a] Yuri Ando,[b] Sohei Nakagawa,[b] Harumitsu Nishikawa,[a] and Takashi Shirai *[ab]

We have previously reported the effective catalytic decomposition of volatile organic compounds (VOC) using stoichiometric hydroxyapatite (HAp), making it as the most promising alternative catalyst to replace the expensive conventional noble-metal nanoparticles for VOC purification. Here we derive a catalysis mechanism by exploring HAps of variable Ca/P molar ratios (1.70, 1.67, 1.57, 1.37) for the catalytic decomposition of VOCs (ethyl acetate, isopropanol, acetone). In particular, the mechanism is discussed with respects to particle morphology, specific surface area, crystallinity, chemical structure, radical generation, in-situ VOC adsorption properties and acidic/basic sites population of HAps combined with confirmation of decomposed by-products in different VOCs. The achieved nearly total decomposition (98.04%) of VOCs and the initially established catalysis mechanism demonstrated in this work not only provide principle information for catalysis science and technology, but also open new possibility for the design of noble-metal-free catalyst towards environmental cleaning.

Introduction

Controlling emission of volatile organic compounds (VOC) emission acting as precursors of ozone and photochemical smog which causes serious air and water pollution is one of the main issues for global environmental purification and protection in decades. VOC also has short- and long-term health effects due to their malodorous, mutagenic and carcinogenic nature.[1-3] The conventional control processes involve condensation,[4] adsorption,[5] biological degradation, [6] plasma assisted decomposition,[7] photo- and thermal-catalytic oxidation[8-10] are established. Thermal-catalytic oxidation has attracted much attention due to the low reaction temperature and efficient destruction of VOCs into harmless CO_2 and water. Noble-metal nanoparticles (NPs), such as platinum (Pt) and palladium (Pd) NPs, supported on mesoporous ceramic filters are the most utilized system for the catalytic decomposition of industrial VOCs.[8,10] With regards to the high-cost and strict dispersibility requirement of NPs, development of alternative and new type catalyst for VOC decomposition is desired to achieve sustainable goals in delivering affordable and clean energy, clean water as well as climate action.

We have initially reported an efficient catalytic decomposition of VOCs using stoichiometric hydroxyapatite (HAp).[11,12] HAp, as one of the most well-known calcium phosphate materials attracting world attention in applications towards bio-ceramics, adsorbents, ion-exchanging fillers and catalyst supports due to its excellent biocompatibility, non-toxicity and chemical stability.[13-16] Besides the above properties, we focused on the radical generation on HAp surface during thermal treatment. With thermally dehydration of P-OH, the electrons trapped in vacancies will continuously react with surface adsorbed oxygen molecular and generate oxygen radical. Such super oxygen radicals are supposed to be active for the catalytic decomposition of VOCs, which makes HAp as the most promising material to replace noble-metal NPs catalysts due to the advantages as low-cost and supporting material free. [11,12,17] In previous study, we investigated the catalytic decomposition of VOCs on stoichiometric HAp by evaluating the CO, CO_2 conversions ability.[11] We also demonstrated the influence of crystal structure on catalytic activity of HAp with comparison of two kinds of HAps with preferred crystal growth along a- and c-axes, respectively.[12] However, the catalytic mechanism has not been clarified due to lack of detailed characterizations of HAp and confirmation of by-products except than CO, CO_2. Herein, the catalytic decomposition of different VOCs (ethyl acetate, isopropanol, acetone) on HAp with varied Ca/P molar ratios (1.70, 1.67, 1.57, 1.37) are investigated. The mechanism of catalytic reactions is systemically discussed with detailed characterizations of particle morphology, specific surface area, crystallinity, chemical structure, radical generation, in-situ adsorption/desorption properties and acidic/basic sites evaluation of HAps combined with confirmation of decomposed by-products in different VOCs and HAps systems. The observed nearly total decomposition of VOCs on selected HAps and the initially clarified catalysis mechanism demonstrated in this work not only provide principle information for catalysis science and technology, but also open new possibility for the design of

[a] Advanced Ceramics Research Center, Nagoya Institute of Technology, Gokiso-cho, Showa-ku, Nagoya, Aichi, Japan 466-8555.
[b] Department of Life Science and Applied Chemistry, Graduate School of Engineering, Nagoya Institute of Technology, Gokiso-cho, Showa-ku, Nagoya, Aichi, Japan 466-8555.

† Footnotes relating to the title and/or authors should appear here.
Electronic Supplementary Information (ESI) available: [details of any supplementary information available should be included here]. See DOI: 10.1039/x0xx00000x

noble-metal-free catalyst for pollution control and environmental cleaning technologies.

Experimental

Materials and methods

Four kinds of HAp samples of different Ca/P molar ratios of 1.70, 1.67, 1.57 and 1.37 were provided by Taihei Chemical Industrial Co., Ltd and utilized in this work.

For catalytic decomposition of VOC, ethyl acetate, isopropanol and acetone gases are prepared via a permeator system (PD-1B-2, GASTEC Corp.) under controlled temperatures. The concentration of each VOC is controlled as 100 ppm by dilution with continuous N_2 flow. A mixture flow of VOC and air with molar ratio of 1:1 in a quartz reaction tube with HAp powders loaded, during where the temperature is controlled by an electrical furnace as reported previously. The reacted gases are collected in sample bags for further characterizations.

Characterizations

The morphology and size of HAp powders were confirmed by scanning electron microscope (SEM: JCM-6000 NeoScope, JEOL Ltd). The crystallinity of raw and thermally treated HAp powders was confirmed by powder X-ray diffraction equipment (XRD: Ultima IV, Rigaku Corp.) equipped with Cu Kα and operating current/voltage of 40 mA/40 kV. The specific surface area (SSA) of HAp is evaluated on a commercial nitrogen adsorption/desorption system of BET method (BELSORP miniX, MicrotracBEL Corp.). The generation of active radicals under different temperatures is analysed by an electron spin resonance instrument equipped with in-situ heating system (ESR: JEOL Ltd). As for the characterization of surface interaction between VOC and HAp, a Fourier transform infrared spectroscopy (FTIR: FT/IR-6000, JASCO Corp.) equipped with in-situ diffuse reflectance chamber is utilized, which has been demonstrated in our previous paper.[10] For quantity of acidic site and basic site population on HAps surface, a commercial absorption/desorption system (BELSORP maxII-SE, MicrotracBEL Corp.) with ammonia (NH_3) / carbon dioxide (CO_2) gases flow is applied. In the case of gas generation evaluation in VOC decomposition experiments, the concentration of CO and CO_2 products are detected by a commercial infrared absorption CO (UM-300: KITAGAWA KOMYO RIKAGAKU KOGYO) and CO_2 (RI-215D: RIKEN KEIKI Co., Ltd.) monitors, while organic by-product components are analysed by gas chromatography with flame ionization detector (GC: GC2030, Shimazu Corp.) and GC mass spectroscopy (GC-MS: GCMS-QP2010SE, Shimazu Corp.). The initial and residual concentration of VOC before and after decomposition is estimated through pre-measured calibration curve in GC measurement. Then, the conversion of VOC is calculated via following equation:

$$Coversion\% = \frac{VOC\ Concentration_{\ initial} - VOC\ Concentration_{residual}}{VOC\ Concentration_{\ initial}} \times 100\%.$$

The CO_2 selectivity is further calculated based on following equation, where N_{Carbon} represents the total number of carbon atom in VOC molecular:

$$Selectivity_{CO_2}\% = \frac{Concentration_{CO_2}}{N_{Carbon} \times VOC\ Concentration_{initial} \times Conversion\%} \times 100\%.$$

Results and discussion

Characterization of HAp powders

Fig. 1 shows the FE-SEM images of received HAp powders with Ca/P ratio of 1.70, 1.67, 1.57, 1.37 (named as HAp-1.70, HAp-1.67, HAp-1.57 and HAp-1.37 respectively). Aggregations of nano-ordered primary particles are observed in all HAp samples, where the size of primary particles is smaller in HAp-1.67 and HAp-1.57. The SSA of HAp-1.70, HAp-1.67, HAp-1.57 and HAp-1.37 analysed by BET method are 31.60, 72.05, 60.67 and 48.74 m^2/g, respectively, whose results show good correlation with particle size observed in SEM images. Fig. 2 demonstrates the XRD patterns of raw HAp powders, where monocrystalline phase of HAp is confirmed in all samples. HAp-1.70 and HAp-1.67 exhibits higher crystallinity than HAp-1.57 and HAp-1.37 according to the narrow peaks with small FWMH (full width of maximum half) value based on Sherer's equation.

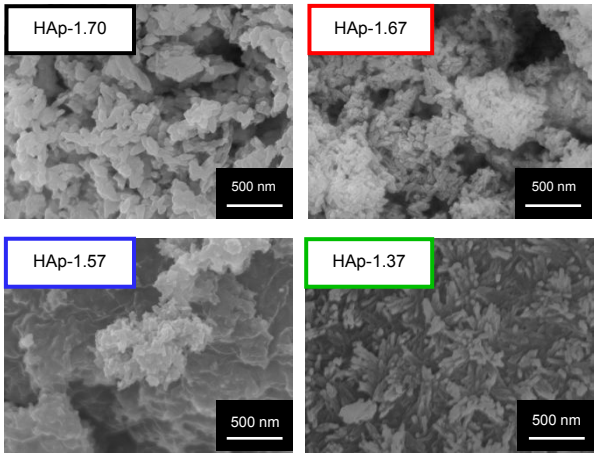

Fig. 1. SEM images of observed HAp powders with Ca/P molar ratio of (a) 1.70, (b) 1.67, (c) 1.57 and (d) 1.37.

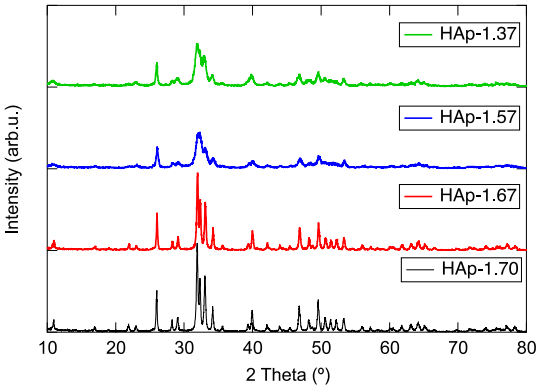

Fig. 2. PXRD patterns of received HAp powders.

Catalytic decomposition of ethyl acetate on HAps

The chemical components analysed via GC in gaseous ethyl acetate before and after catalytic decomposition at 400°C is shown in Fig. 3 (a). Peaks of ethylene (C_2H_4), acetaldehyde (CH_3CHO) and ethanol (C_2H_5OH) identified with assistance of GC-MS, as by-products are clearly obtained in decomposed gas samples of HAp-1.70 and HAp-1.67. Ethylene is copiously observed for HAp-1.57 sample while the existence of acetaldehyde is minor. In the case of catalytic decomposition on HAp-1.37, acetaldehyde is not detected and a large peak of residual ethyl acetate is confirmed. To compare the catalytic activity for ethyl acetate decompaction over different HAps, the conversion efficiencies are summarized as a function of temperature in Fig. 3 (b). It can be clarified that the decomposition starts from 250°C and reach the maximum value at 400°C in all HAps. It is worth noting that nearly total decomposition with conversion efficiency of 98.04 % is successfully achieved in HAp-1.67. The maximum catalytic activity is in the order of HAp-1.67>HAp-1.70>HAp-1.57>HAp-1.37, while HAp-1.57 seems to give more efficient decomposition in the low temperature region.

In order to clarify the reason of catalytic activity difference, radical generation at 400°C was characterized via in-situ ESR and the results are displayed in Fig. 4. As indicated by Fig. 4 (a), signal with g value of 2.003 corresponding to trapped electron which relates to the oxygen radical formation appears in HAp-1.67 and HAp-1.70 samples, whose value is shifted to 2.002 in Ca-deficient HAp-1.57 and HAp-1.37.[11,12,17] To quantifying the generated amount of oxygen radicals on total surface area, the intensity ratio between signal and Mn marker is calculated and illustrated as Fig. 4 (b). It suggests that the most radicals are generated on HAp-1.70, which is higher than HAp-1.57, HAp-1.67 and HAp-1.37. Such tendency is partially correlated well with the catalytic activity results given by Fig. 3 (b) except HAp-1.70 and HAp-1.57, which perform higher radical generation but lower catalytic activity than HAp-1.67.

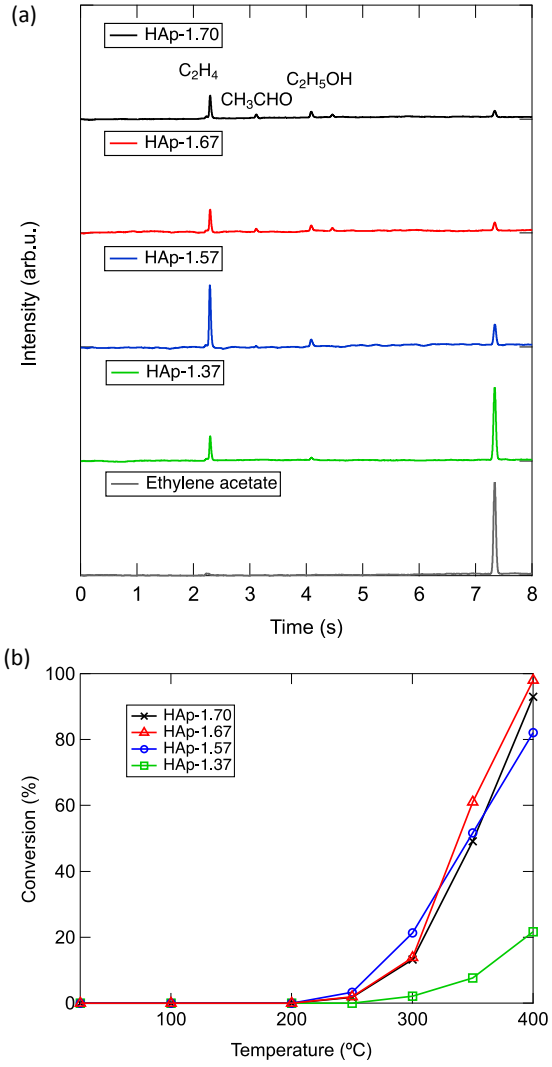

Fig. 3. (a) GC spectra of ethyl acetate before and after catalytic decomposition on HAp powders at 400°C (b) Calculated conversion efficiency of ethyl acetate on HAp powders as a function of temperature.

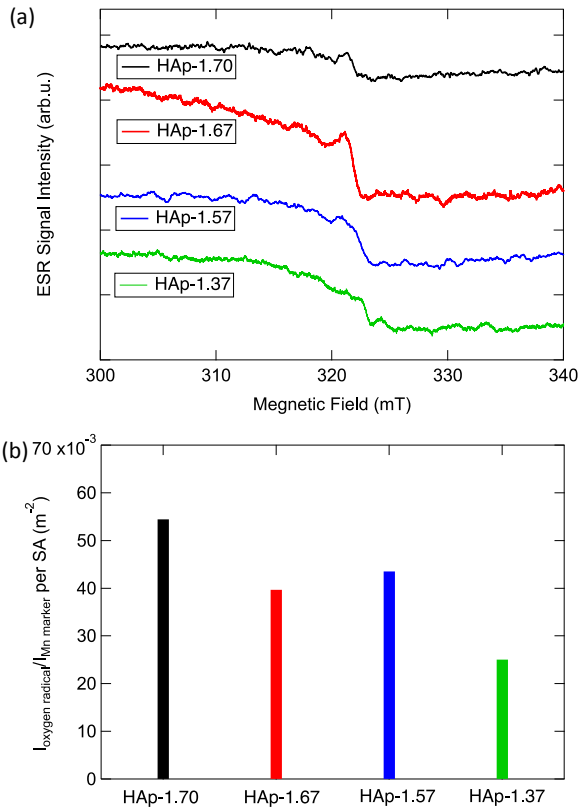

Fig. 4. (a) In-situ ESR spectra and (b) Calculated intensity ratio of $I_{oxygen\ radial}/I_{Mn\ marker}$ per surface area for different HAp powders at 400°C.

We consider other factors such as adsorption property of VOC on HAp might also has an effect on the catalytic decomposition performance. Thus, the adsorption of ethylene acetate is analysed via an in-situ FT-IR system equipped with continuous flow of ethyl acetate, whose construction has been reported in our previously paper. As FT-IR spectra shown in Fig.

5 (a), the O-H stretching mode of apatite hydroxyl group is identified as a sharp peak appears at 3570 cm^{-1}. Multiple peaks at 1950-2150 cm^{-1} correspond to combination and overtone mode of PO_4^{3-}.[18,19] The peak around 1570 cm^{-1} appears in spectra of HAp-1.37 can be attributed to substituted CO_3^{2-} ions generated during synthesis process. The peak observed around 1750-1650 cm^{-1} originates from the absorption of C=O bond in ethyl acetate on HAps surface.[12,20] The amount of adsorbed ethyl acetate on different HAp is compared by calculating the peak intensity ratio of C=O/PO_4^{3-}. As indicated by Fig. 5 (b), deficient HAps show higher adsorption amount on surface than stoichiometric and Ca-rich HAps. Such phenomenon can be attributed to the enriched charge on surface in deficient HAps which results in stronger interaction between C=O and enhanced adsorption. Regards to the radical generation results given by Fig. 4 (b), it can be considered that the lower catalytic activity of HAp-1.70 for decomposition of ethylene acetate must be due to the lower adsorption amount of ethyl acetate on surface despites a better radical generation. Thus, we conclude that catalytic activity is not only depend on the radical generation on HAp surface but also the interaction with VOC. Since HAp-1.57 exhibits better radical generation and VOC adsorption abilities but low catalytic activity than HAp-1.67, we suggest other chemical structure induced reactions might have an influence on the catalytic activity of HAp-1.57 and continue the investigation step by step also in following parts.

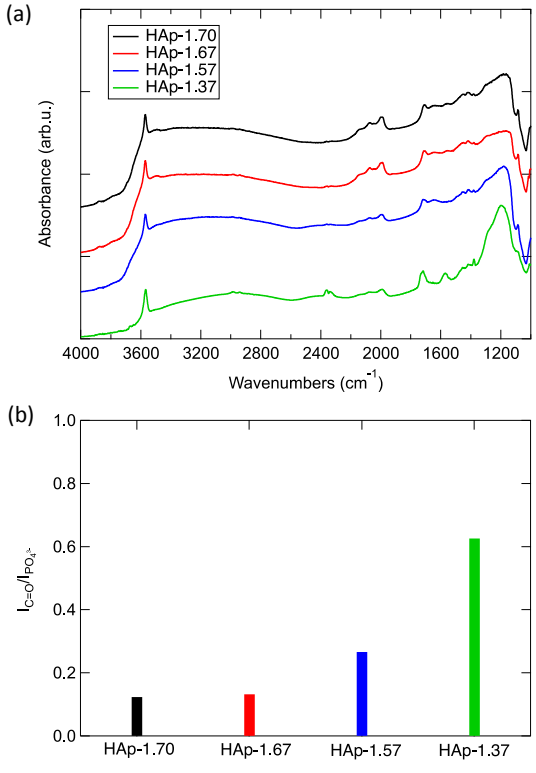

Fig. 5. (a) In-situ FTIR spectra and (b) Calculated intensity ratio of $I_{C=O}/I_{PO4}^{3-}$ for different HAp powders.

Catalytic decomposition of isopropanol on HAps

According to the generation of alcohol as by-product in decomposition of ethyl acetate, we choose isopropanol for the discussion of alcohol which emitted significantly in manufacturing process as one of the main VOC sources. The GC spectra of isopropanol before and after decomposition on different HAps are illustrated in Fig. 6 (a). In addition to initial spectra of isopropanol, peaks corresponding to propylene (CH_2CHCH_3) and acetone (CH_3COCH_3) are detected in HAp decomposed gases. In the case of stoichiometric (HAp-1.67) and Ca-rich (HAp-1.70) HAps, the peaks of propylene and acetone show equivalent intensity, while propylene peak exhibits much higher density in deficient HAps (HAp-1.57 and HAp-1.37).

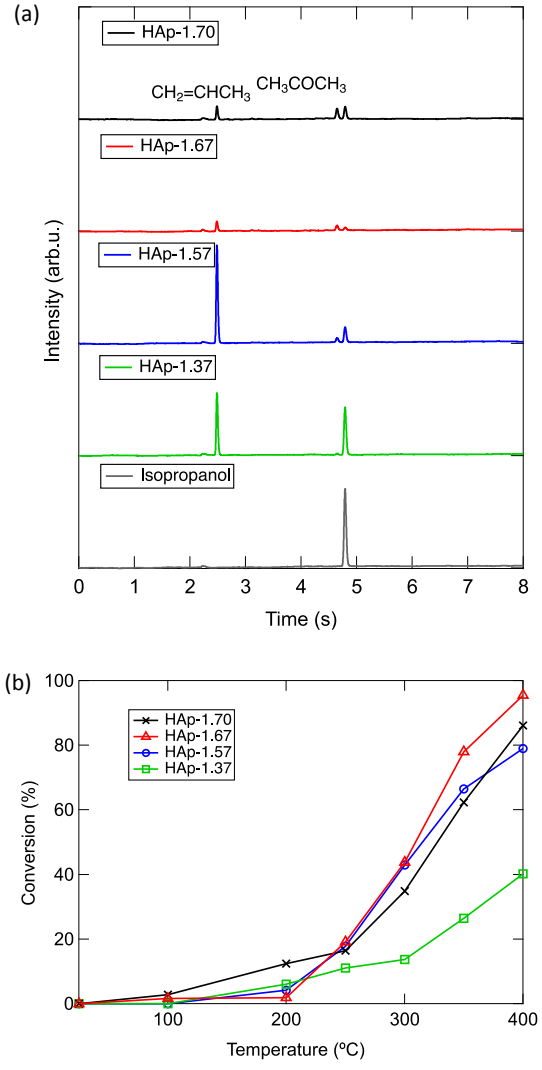

Fig. 6. (a) GC spectra of isopropanol before and after catalytic decomposition on HAp powders at 400°C (b) Calculated conversion efficiency of isopropanol on HAp powders as a function of temperature.

As results given in Fig. 6 (b), it can be demonstrated that the decomposition of isopropanol starts from lower temperature region

(T=200°C ~) than ethyl acetate. Since there is no radical detected under 200°C,[11] we proposed other reaction mechanism must be included in decomposition process. By considering HAp exhibits both acid and base characteristics, the amount of acidic and basic sites on HAp surfaces are evaluated with assistance of an adsorption and desorption system using ammonia (NH_3) and carbonate (CO_2) gases.[21] As calculated results given in Table 1, 46% acidic site and 54% basic site exist on HAp-1.70 surface and the percentage of acidic site increases as Ca/P ratio decreases. Regards to the fact that acidic site on HAp surface are considered as Ca^{2+}, HPO_4^{2-}, while basic site can be induced by PO_4^{2-} and OH^-, our calculated results show good agreement that population of acidic site increases in HAp-1.70 due to increased amount of Ca^{2+}. For HAp-1.57, the populated acidic sites can be attributed to the exitance of HPO_4^{2-} with reduced PO_4^{2-} and OH^-. In the case of HAp-1.37, the harvested acidic sites are originated from the substitution of PO_4^{2-} and OH^- into CO_3^{2-}. By correlating with VOC decomposition results given by Fig. 6, it can be concluded that HAps with more basic site on surface such as HAp-1.70 and HAp-1.67, oxidation is more promoted and acetone is generated, while dehydrogenation with production of propylene takes place mainly in deficient HAps with more acidic site as HAp-1.57 and HAp-1.37.[21] Thus, we conclude that the decomposition of VOCs consists hydroxyl-group as isopropanol, not only the active radicals but also the acidic and basic sites existed on HAps surface play an important role in the catalytic reaction and conversion efficiency.

Table 1. Absorption amount of NH_3 and CO_2 on different HAp powders and calculated percentage of acid-/base-site.

Sample	NH_3	CO_2	Population [%]	
	[μmol/m²]	[μmol/m²]	Acidic site	Basic site
HAp-1.70	0.27	0.23	54	46
HAp-1.67	0.12	0.53	18	82
HAp-1.57	0.70	-	100	0
HAp-1.37	0.20	-	100	0

Catalytic decomposition of acetone on HAps

With respect to the appearance of C=O consisted molecules as by-product in the catalytic decomposition of ethyl acetate and isopropanol, the decomposition of acetone on different HAps is investigated. Fig. 7 (a) and (b) shows the GC spectra of acetone before and after decomposition and calculated conversion efficiency, respectively. As indicated by Figure 7 (a), no by-product was detected in all samples which proves that no further reaction between HAp and acetone. The highest conversion efficiency was observed in stoichiometric HAp, while HAp-1.70 and HAp-1.57 show medium conversion efficiency and HAp-1.37 gives the lowest catalytic ability.

Here we initially propose the catalytic decomposition mechanism of VOCs on HAp in this paper as following based on the above results and discussion. In the case of ethyl acetate, it is decomposed into acetaldehyde and ethanol through reaction with thermally activated radicals on HAp surface as first step reaction. Secondly, the generated ethanol reacted on acidic (HPO_4^{2-}, Ca^{2+}) and basic (PO_4^{3-}, OH^-) sites on HAp surface, which produce ethylene and acetaldehyde through dehydrogenation and oxidization reaction, respectively. Such process can be well supported by the catalytic decomposition result of isopropanol on HAp. Thirdly, the produced acetaldehyde continuously converted into CO_2 and CO with assistance of super active radicals, whose conclusion can be confirmed by the GC results of acetone decomposition. The above three-step catalytic decomposition process is illustrated as Scheme 1. Thus, the catalytic activity of HAp in VOC decomposition must be decided by the radical generation, VOC adsorption, as well as surface acidic/basic properties, which are strongly influenced by the chemical structure of HAp. In addition, we suggest the above

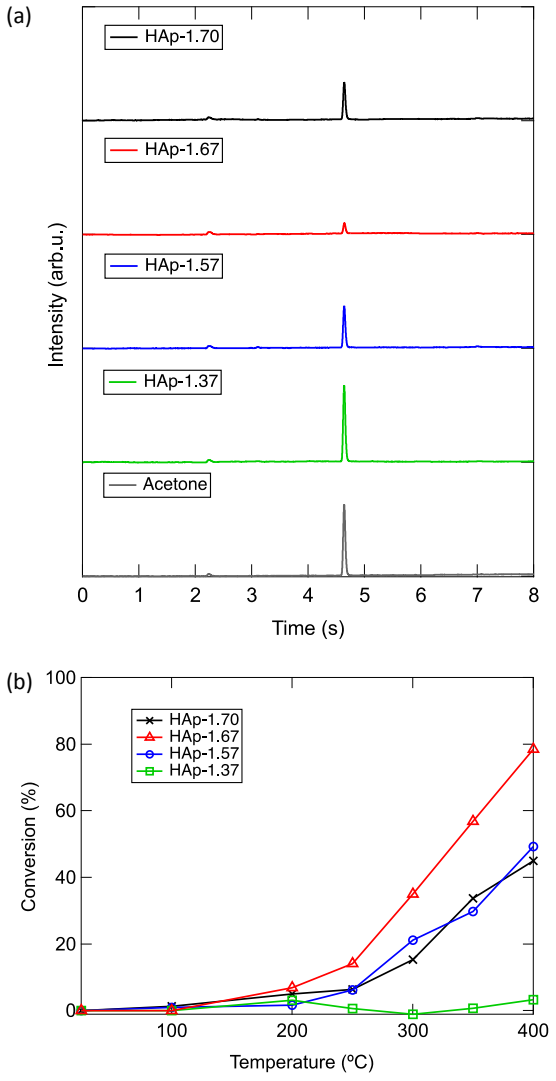

Fig. 7. (a) GC spectra of acetone before and after catalytic decomposition on HAp powders at 400°C (b) Calculated conversion efficiency of acetone on HAp powders as a function of temperature.

mechanism can be adapted in the catalytic decomposition of acetate, alcohol, aldehyde and ketone molecules.

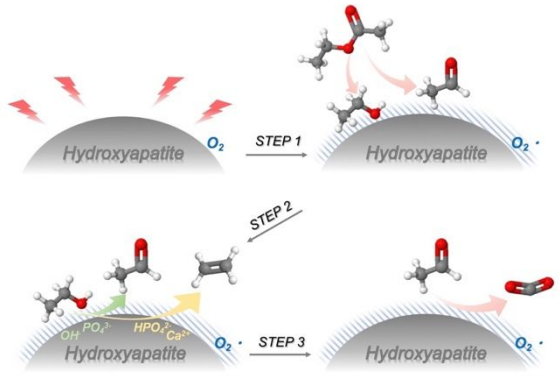

Scheme 1. Catalytic reaction mechanism of ethyl acetate decomposition on HAp.

CO_2 selectivity of different HAps

The obtained CO_2 selectivity of different HAps at 400°C are summarized in Fig. 8 as appendix information of this study. As a result, HAp-1.67 performs the highest CO_2 selectivity in catalytic decomposition of ethyl acetate, isopropanol and acetone, while HAp-1.37 show almost zero CO_2 selectivity. In the case of acetone, the CO_2 selectivity must be significantly influenced by radical generation on HAp and adsorption property of acetone based on the suggested reaction mechanism above. For the same reason, the CO_2 generation in isopropanol decomposition significantly depends on the amount of acetone as by-product in first step catalytic reaction. That is, higher CO_2 selectivity can be obtained in HAp-1.70 and HAp-1.67 which produce more aldehyde/acetone due to harvested basic sites of OH- and PO_4^{3-}. We believe the CO_2 selectivity in both of alcohol and aldehyde/ketone decompositions contributes to that of ethyl acetate case. Although the CO_2 selectivity is near 60% at 400°C, such value is estimated approach to 100 % at 500°C in our previously report and thus the total decomposition of VOCs into CO_2 can be also expected at higher temperature range.

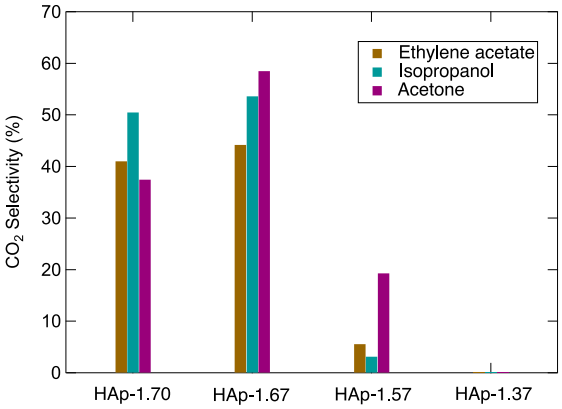

Fig. 8. Calculated CO_2 selectivity of different HAps in catalytic decomposition of ethylene acetate, isopropanol and acetone at 400°C.

Conclusions

In this work, the catalytic decomposition of different VOCs (ethylene acetate, isopropanol, acetone) on HAp with varied Ca/P molar ratios (1.70, 1.67, 1.57, 1.37) are investigated. As a result, stoichiometric HAp performs the highest catalytic activity towards the decomposition of VOCs. Nearly total decomposition of ethylene acetate and isopropanol is achieved at 400°C, whose value is near 80% in the case of acetone. Ca-rich (HAp-1.70) and deficient (HAp-1.58) HAps exhibit lower conversion efficiency, and HAp-1.37 gives the worst catalytic performance. Based on the characterization results of radical generation, VOC adsorption property, acidic and basic sites evaluation of HAps, as well as detailed GC and GC-MS analysis of decomposed gases, the catalytic reaction mechanism on HAp with different Ca/P molar ratio is clarified. For the decomposition of acetate, it can be decomposed into alcohol and ketone through reaction with thermally induced radicals on HAp surface. Alcohol can be further dehydrated on acidic site (HPO_4^{2-}, Ca^{2+}) and oxides on basic site (PO_4^{3-}, OH^-) to produce alkene and ketone, where ketone is continuously converted into CO_2 and CO. We suggest the catalytic activity of HAp in VOC decomposition must be decided by the radical generation and VOC adsorption properties, as well as surface acidic/basic properties simultaneously. We believe the results in this paper not also provide principle information of catalytic reaction mechanism of HAp towards decomposition of VOC but also open new possibility for the material design of noble-metal-free catalyst for environmental purification technologies.

Conflicts of interest

There are no conflicts to declare.

Acknowledgements

This work is supported in part by A-STEP (Adaptable and Seamless Technology Transfer Program through Target-driven R&D) of JST (Japan Science and Technology Agency).

References

1 P. M. Lemieux, C. C. Luters and D. A. Santoianni, *Prog. Energ. Comb. Sci.,* 2004, **30**, 1-32.
2 M. Placet, C. O. Mann, R. O. Gibert and M. J. Niefer, *Atmosp. Envir.,* 2000, **34**,2183-2204.
3 Y. Huang, S. S. H. Ho, Y. Lu, R. Niu, L. Xu, J. Cao and S. Lee, *Molecules,* 2016, **21**, 56.
4 R. F. Dunn and M. M. El-Halwagi, Waste Manag., 1994, **14**, 103-113.
5 X. Zhang, B. Gao, A. E. Creamer, C. Cao and Y. Li, *J Hazard Mater.,*. 2011, **192** (2): 683-90.
6 M. Yoshikawa, M. Zhang and K. Toyota, *Microbes Environ.,* 2017, **32**, 188-200.
7 X. Feng, H. Liu, C. he, Z. Shen and T. Wang, *Catal. Sci. Tech.,* 2018, **8**, 936-954.
8 V. Hequet, C. Raillard, O. Debono, F. Thevent, N. Locoge and L. Le Cop, *Appl. Catal. B,* 2018, **226**, 473-486.

9 L. F. Loitta, *Appl. Catal. B,* 2010, **100**, 403-412.
10 H. Huang, Y. Xu, Q. Feng and D. Y. C. Leung, *Catal. Sci. Technol.,* 2015, **5**, 2649.
11 H. Nishikawa, T. Oka, N. Asai, H. Simomichi, T. Shirai and M. Fuji, *Appl. Surf. Sci.,* 2012, **258**, 5370-5374.
12 Y. Xin, H. Ikeuchi, J. Soo, H, Nishikawa and T. Shirai, *J. Ceram. Soc. Jpn.,* 2019, **127**, 263-266.
13 K. Lin, C. Wu and J. Chang, *Act. Biomat.,* 2014, **10**, 4071-4102.
14 W. Suchanek and M. Yoshimura, *J. Mater. Res.*, 1998, **13**, 94-117.
15 L. Dong, Z. Zhu, Y. Qiu and J. Zhao, *Chem. Eng. J.,* 2010, **165**, 827-834.
16 T. Kawasaki, *J. Chromatogr. A,* 1991, **544**, 147-184.
17 H. Nishikawa, *Mater. Lett.*, 2001, **50**, 364-370.
18 E. Tkalcec, M. Sauer, R. Noninger and H. Schmidt, *J. Mater. Sci.,* 2001, **36**, 5253-5263.
19 M. M. Beasley, E. J. Baterlink, L. Taylor and R. M. Miller, *J. Mater. Sci.,* 2001, **36**, 5253-5263.
20 Q. Chang, K. K. Li, S. L. Hu, Y. G. Dong and J. L. Yang, *Mater. Lett.,* 2016, **175**, 44-47.
21 S. Ogo, A. Onda, Y. Iwasa, K. Hara, A. Fukuoka and K. Yanagisawa, *J. Catal.,* 2012, **296**, 24-30.

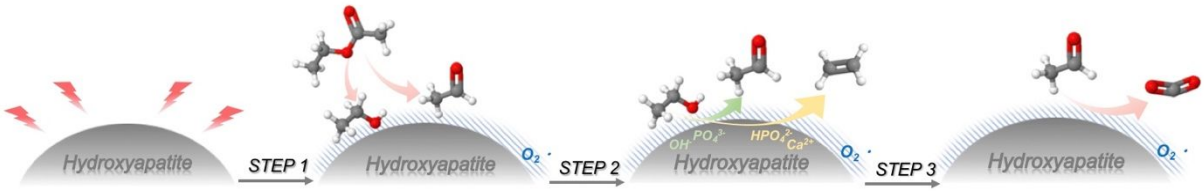

Initially established catalysis mechanism for the decomposition of VOC on noble-metal-free hydroxyapatite catalyst